

Supplement of Atmos. Chem. Phys., 20, 14847–14871, 2020
<https://doi.org/10.5194/acp-20-14847-2020-supplement>
© Author(s) 2020. This work is distributed under
the Creative Commons Attribution 4.0 License.



Supplement of

Elevated levels of OH observed in haze events during wintertime in central Beijing

Eloise J. Slater et al.

Correspondence to: Dwayne E. Heard (d.e.heard@leeds.ac.uk) and Lisa K. Whalley (l.k.whalley@leeds.ac.uk)

The copyright of individual parts of the supplement might differ from the CC BY 4.0 License.

Supplementary Information

1.1 Effect of deposition rate on the radical concentration and OH reactivity.

The MCM-base model, which uses a deposition rate of 0.1/MH, has been run again using several different deposition rates for the model generated intermediates. The effect of changing the deposition rate on the concentration of OH, HO₂ and RO₂, and also on the OH reactivity, kOH, is shown in Figure S1. Figure S1 shows that changing the deposition rate does not change the radical concentration significantly (less than 5%), and for the OH reactivity the maximum difference is 10%. The small changes in OH reactivity when the deposition rate is changed by a factor of 10 shows that the model intermediates do not contribute significantly to the OH reactivity, rather the OH reactivity is dominated by measured, primary emissions. It also shows that the deposition rate used in the MCM-base model run is appropriate as the OH reactivity is replicated well, and changes in the deposition rate do not change the total radical concentration significantly.

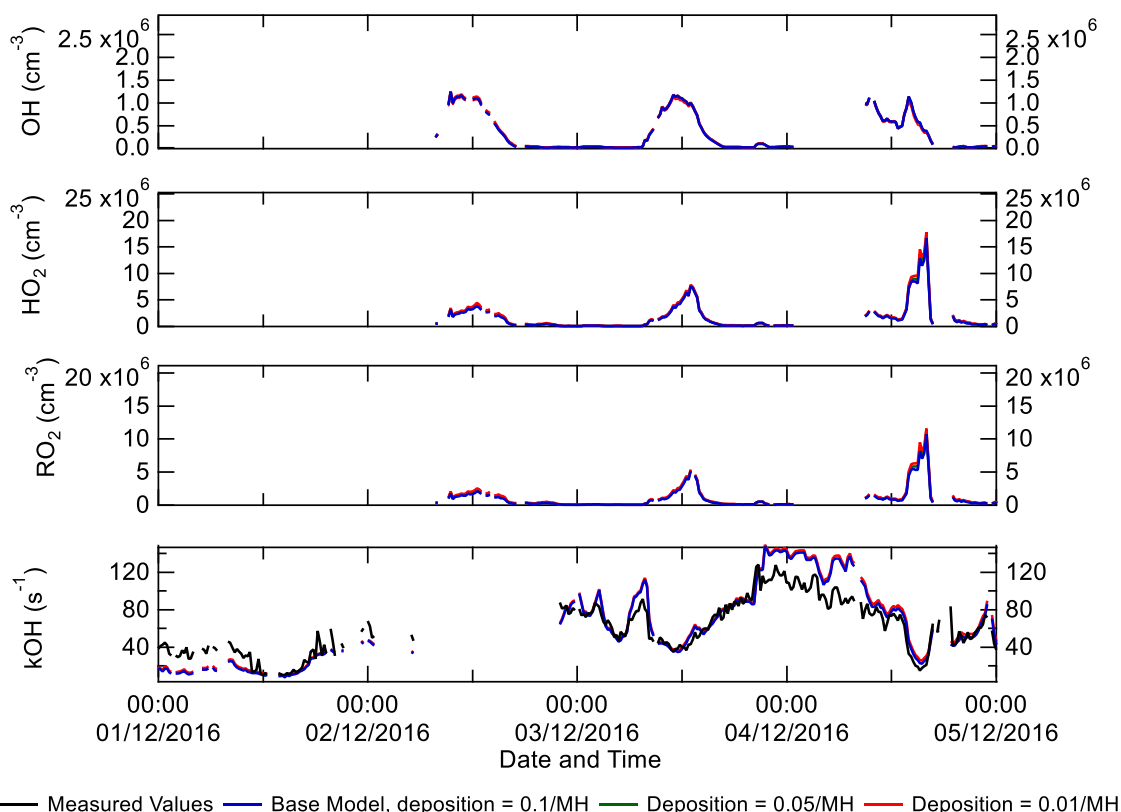


Figure S1. Effect of changing the deposition rate for model generated intermediates on the concentrations of OH, HO₂ and RO₂, and the OH reactivity, together with a comparison with the measurements.

For the winter campaign only, VOC species up to C₇ were measured by the DC-GC-FID, but to test the sensitivity of the model to higher weight VOCs, measurements from a PTR-MS were incorporated into the MCM-base model to include C₂ and C₃ aromatic species. The species measured by the PTR-MS

and used in this model run, MCM-fVOC, were ethyl benzene(C2), propyl benzene(C3), isopropyl benzene(C3), 2-Ethyltoluene(C3), 3-Ethyltoluene(C3), 4-Ethyltoluene(C3), 1,3,5-trimethylbenzene(C3), 1,2,4-trimethylbenzene(C3) and 1,2,3-trimethylbenzene (C3). Since the DC-GC-FID measured three C2 aromatic species (o-xylene, m-xylene and p-xylene) the concentration of ethyl benzene was calculated through the difference between the PTR C2 and the DC-GC-FID C2 measurements. The model comparison between MCM-base and MCM-fVOC model runs is shown in Figure S2, and shows that introducing higher weight VOCs does not effect the radical concentration significantly, with the largest difference observed on the 5/12/2016 of ~7%.

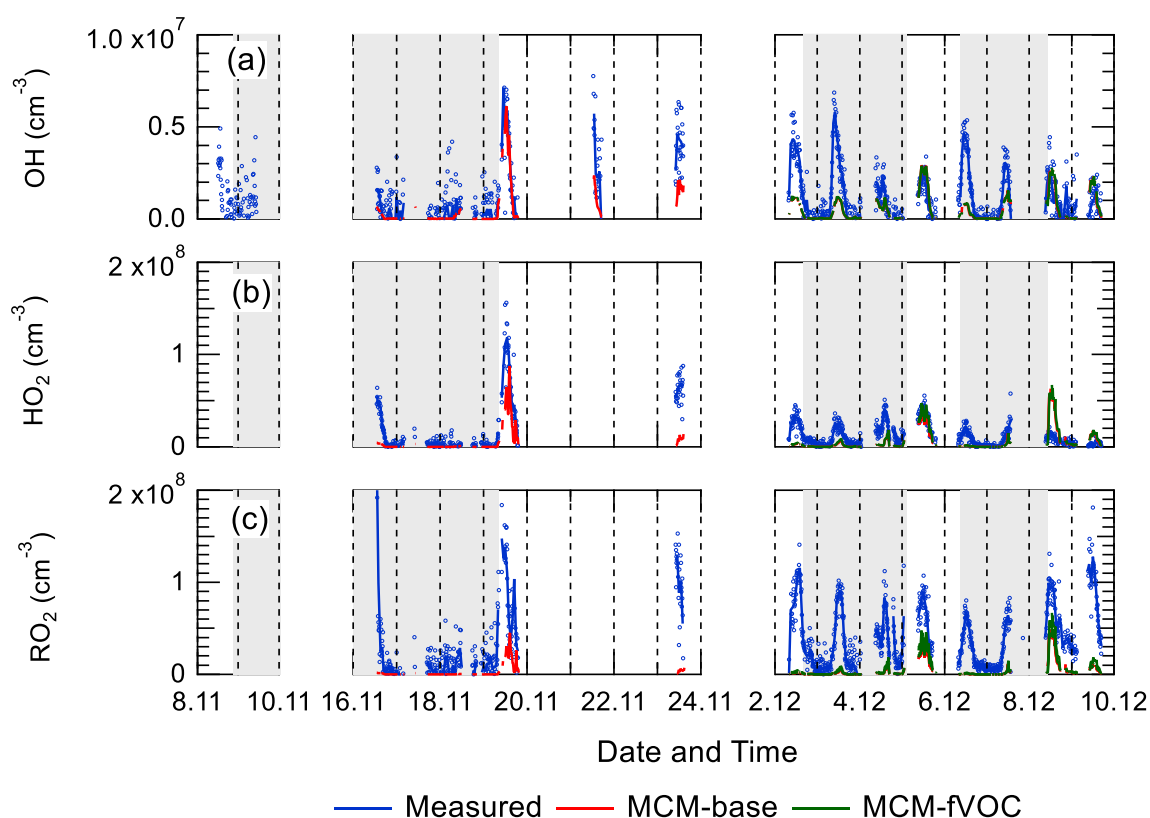


Figure S2 a) Comparison of measured OH with modelled OH from MCM-base and MCMfVOC. b) Comparison of measured HO₂ with modelled HO₂ from MCM-base and MCM-fVOC. c) Comparison of measured total RO₂ with modelled total RO₂ from MCM-base and MCMfVOC. It should be noted that PTR-MS data were only available from 24/11/2016 onwards, hence the data comparison is only between the 02/12/2016 – 10/12/2016.

The impact of the higher weight VOCs in the model on OH reactivity is shown in Figure S3, and shows that introducing the higher weight VOCs has a very small impact on modelled kOH, ³ Also the modelled kOH from the MCM-fVOC model run is in good agreement with measured kOH. These results show that the MCM-base model does not have a large sensitivity to the introduction of higher weight aromatic species.

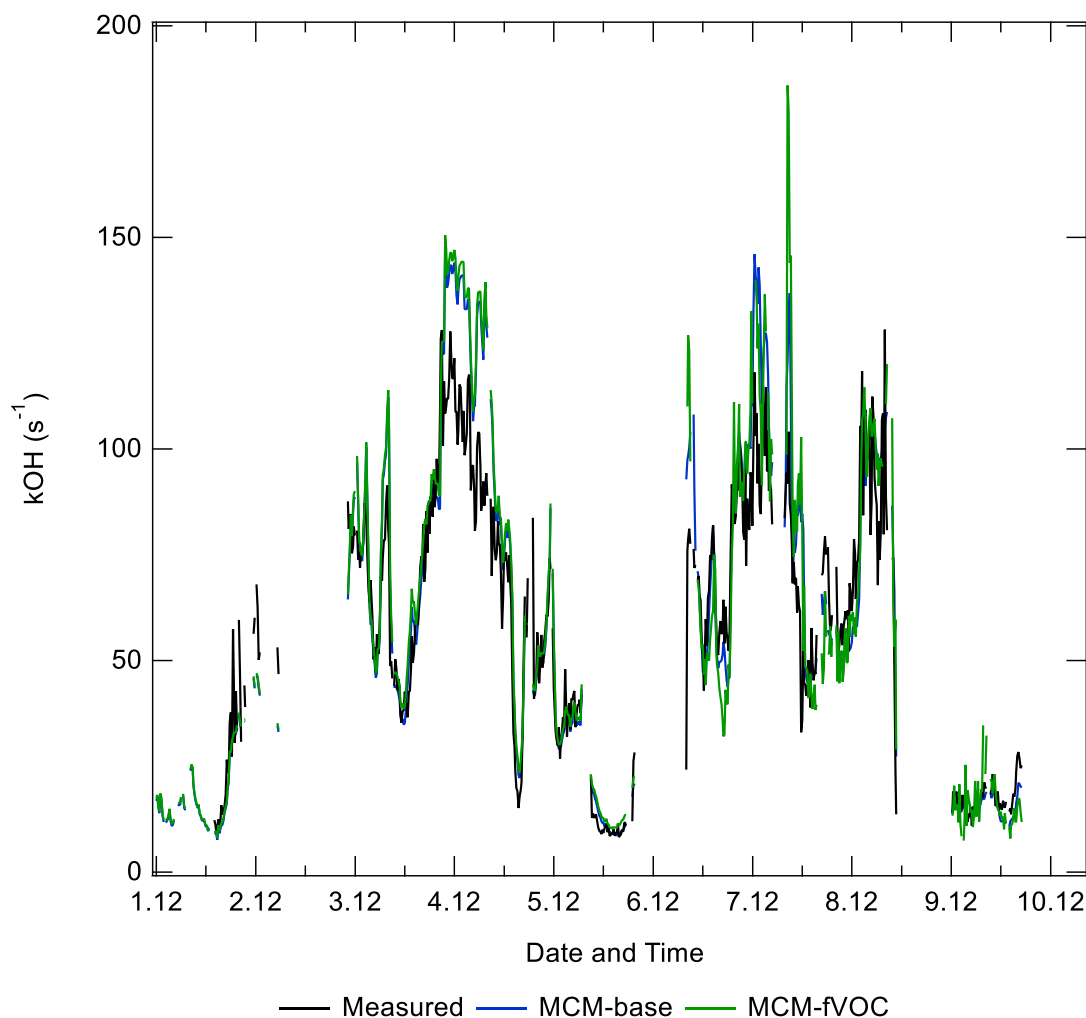


Figure S3. Comparison of measured OH reactivity (kOH) with modelled OH reactivity from the model runs MCM-base and MCM-fVOC.

S1.2 Primary radical production and comparison with previous campaigns.

As summarised in Table S1, several other winter-time campaigns have highlighted the importance of HONO, including the PUMA campaign (Emmerson et al., 2005) in Birmingham; the IMPACT campaign in Tokyo (Kanaya et al., 2007); the NACHTT campaign in Boulder (Kim et al., 2014) and the PMTACS-NY campaign in New York (Ren et al., 2006). These campaigns showed 36.2, 19, 80.4, and 46 % contribution to primary production of RO_x from HONO. However, it should be noted that HONO was not measured during the PUMA campaign, so the percentage contribution to the primary production of radicals should be considered a lower limit as it is based upon modelled HONO (where only the reaction of OH + NO was considered), which is often an underestimate (Lee et al., 2015). As shown in Table 5, the Birmingham, Tokyo, New York and Suburban Beijing campaigns all show a high contribution towards RO_x production from ozonolysis, 63, 35, 42 and 28%, respectively, only the campaign in Boulder (5%) showed little contribution, which is similar to the observations made during APHH campaign. The Boulder campaign is the only one that showed a significant contribution (14.9 %)

to primary radical production from the reaction of $O(^1D) + H_2O$, whilst other winter campaigns show a contribution of less than 1%. The higher contribution from photolysis of O_3 during the Boulder campaign may be due to the campaign taking place in late February (spring) and, as shown in Table S1, photolysis rates, water vapour and temperature were all higher.

	PUMA, Birmingham, UK	IMPACT, Tokyo, Japan	NACHTT, Boulder, USA	PMTACS- NY, New York, USA	BEST-ONE, Suburban Beijing, China	APHH, Central Beijing, China	PKU, Central Beijing, China
Date	Jan – Feb 2000	Jan – Feb, 2004	Late Feb 2011	Jan – Feb, 2001	Jan – March 2016	Nov -Dec, 2016	Jan-Feb, 2017
OH (cm ⁻³)	~1.7 x 10 ⁶	~1.6 x 10 ⁶	~2.7 x 10 ⁶	~ 1.4 x 10 ⁶	3 x 10 ⁶	2.7 x 10 ⁶	1.4 x 10 ⁶
O ₃ (ppbv)	37	20	40	20	30	15	10
<i>j</i> (O ¹ D) (s ⁻¹)	~1 x 10 ⁻⁵	~2.8 x 10 ⁻⁵	~1 x 10 ⁻⁵	~5 x 10 ⁻⁶	7 x 10 ⁻⁶	~3 x 10 ⁻⁶	-
<i>j</i> (O ₃) (%)	0.6	<1	14.7	1.1	<1	<1	<1
<i>j</i> (HONO) (%)	36.2 ^[1]	19	80.4	65.5	46	68	86
Ozonolysis (%)	63.2	35	4.9	42.4	28	21	6
<i>j</i> (Carbonyls) (%)	22	23	-	-	9	8	7% ^[2]
<i>j</i> (HCHO) (%)	6	10	-	6	9	2	
Reference	Emmerson et al. (2005)	Kanaya et al. (2007)	Kim et al. (2014)	Ren et al. (2006)	Tan et al. (2018)	This work.	Ma et al. (2019)

Table S1. Summary of some previous measurements of OH, HO₂ and RO₂ that have taken place during the winter, and a summary of the major primary radical sources during these campaigns. All values are the noon average for each campaign. [1] This should be considered a lower limit due to no HONO measurements being made during the campaign. [2] Primary production from the sum of *j*(Carbonyls) and *j*(HCHO)."

S1.3 NO₂ and SO₂ oxidation during haze events

Secondary oxidation products, such as nitric acid and sulphuric acid, which partition to the aerosol phase, are major contributors towards the formation of secondary particulate matter (Huang et al., 2014). The OH measurements enable calculation of the rate of SO₂ and NO₂ oxidation *via* reaction with OH, to form gas-phase species HNO₃ and H₂SO₄. Figure S4 shows that on average 1.5 ppbv/h and 0.03 ppbv/h of gas-phase NO₂ and SO₂ are oxidised to form acidic species, and that the oxidation increases in these haze periods caused by comparable OH concentration in and out of haze and, as shown in Figure S4, an increase in local NO₂ and SO₂ concentrations. NO_x can also be lost in the atmosphere by the formation of N₂O₅ (Evans, 2005) and subsequent hydrolysis, but this is unimportant in Beijing during winter due to the low levels of O₃. The reaction of OH + SO₂ in the gas-phase is the rate-

determining step in the formation SO_4^{2-} , so the H_2SO_4 formed in the gas-phase will partition in the aerosol phase (Barth et al., 2000). H_2SO_4 is effectively a non-volatile gas at atmospheric temperatures, and H_2SO_4 condensation onto pre-existing particles is an irreversible kinetic process (Zaveri et al., 2008). Whilst HNO_3 is a semivolatile species and the gas-particle partitioning is highly sensitive to meteorological conditions including: temperature, RH, particle size distribution, pH and particle composition. If the relative humidity is lower than the deliquescence relative humidity (RH_d), then the HNO_3 that is formed in the gas phase reacts with NH_3 to form ammonium nitrate aerosol (NH_4NO_3):



If the ambient RH exceeds the RH_d then HNO_3 and NH_3 dissolve into the aqueous phase (aq):



To take into account the reversible process, knowledge of the RH_d that marks the transition between the solid and the aqueous phase, and the equilibrium constant, K_p , for the two phase is required (Ackermann et al., 1998). The MADE module (modal aerosol dynamics model for Europe) uses these thermodynamic parameters as given by (Mozurkewich, 1993), resulting in:

$$\ln\left(\frac{\text{RH}_d}{100}\right) = \frac{618.3}{T} - 2.551 \quad \text{S E1}$$

for RH_d and:

$$\ln(K_p) = 118.87 - \frac{24084}{T} - 6.025 \ln(T) \quad \text{S E2}$$

for K_p . SE1 and SE2 shows that nitrate formation is favoured thermodynamically at low temperatures and high relative humidities (Ge et al., 2017). Previous measurements of SO_4^{2-} and NO_3^- made in wintertime Beijing suggests that photochemistry is important in the formation of nitrate aerosol, but not the formation of sulphate (Ge et al., 2017; Sun et al., 2013).

Figure S4 also shows that the gas-phase oxidation of NO_2 increases under haze conditions, showing that nitrate formation is driven by photochemistry in haze events despite the lower photolysis rates. Similar conclusions have been made in Lu et al. (2019) from measurements during the BEST-ONE campaign; with SO_4^- aerosol predominantly driven by aqueous-phase chemistry whilst the production of NO_3^- aerosol from gas-phase oxidation of NO_2 with OH is important. The maximum production rate of HNO_3 observed during the BEST-ONE campaign is the same as the one calculated for the APHH campaign (3 ppbv hr^{-1}). The BEST-ONE campaign assumed all the gas-phase HNO_3 formed partitioned into the aerosol-phase due to the high relative humidity observed during the campaign.

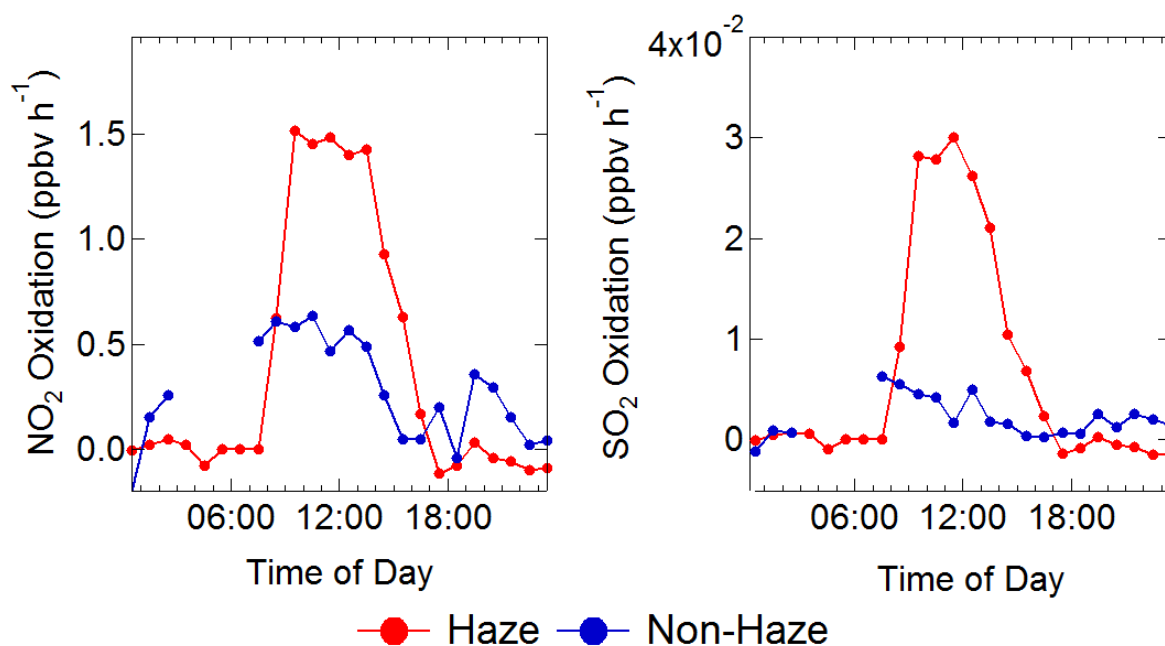


Figure S1. Average diel profiles of the rate of oxidation of NO₂ (left) and SO₂ (right) via reaction with OH in non-haze (blue) and haze (red) conditions.

S1.4 Estimating the contribution of HO₂NO₂ and CH₃O₂NO₂ to the RO₂ signal

In the main paper we do not apply a correction for a possible contribution of pernitric acid (PNA, HO₂NO₂) and methyl peroxy nitric acid (MPNA, CH₃O₂NO₂). The MPNA decomposition will contribute to the simple RO₂ and total RO₂ whilst the PNA contributes to the complex and total RO₂ measurements. The concentration of HO₂NO₂ and CH₃O₂NO₂ was modelled using the MCM-base model, then in agreement with the work by Fuchs et al.(2008) 0.43 % and 9 % of the HO₂NO₂ and CH₃O₂NO₂ is calculated to decompose and contribute to the RO₂ signal. The rate of decomposition in the Julich and Leeds RO_xLIF reactors is expected since the design and residence time (~1 second) are similar. The comparison of the measured total, simple and complex RO₂ with the corrected values is shown in Figure S5. Figure S5 shows that the correction from the decomposition of HO₂NO₂ and CH₃O₂NO₂ is ~6 %, ~8 % and 4 % for total, complex and simple RO₂, respectively.

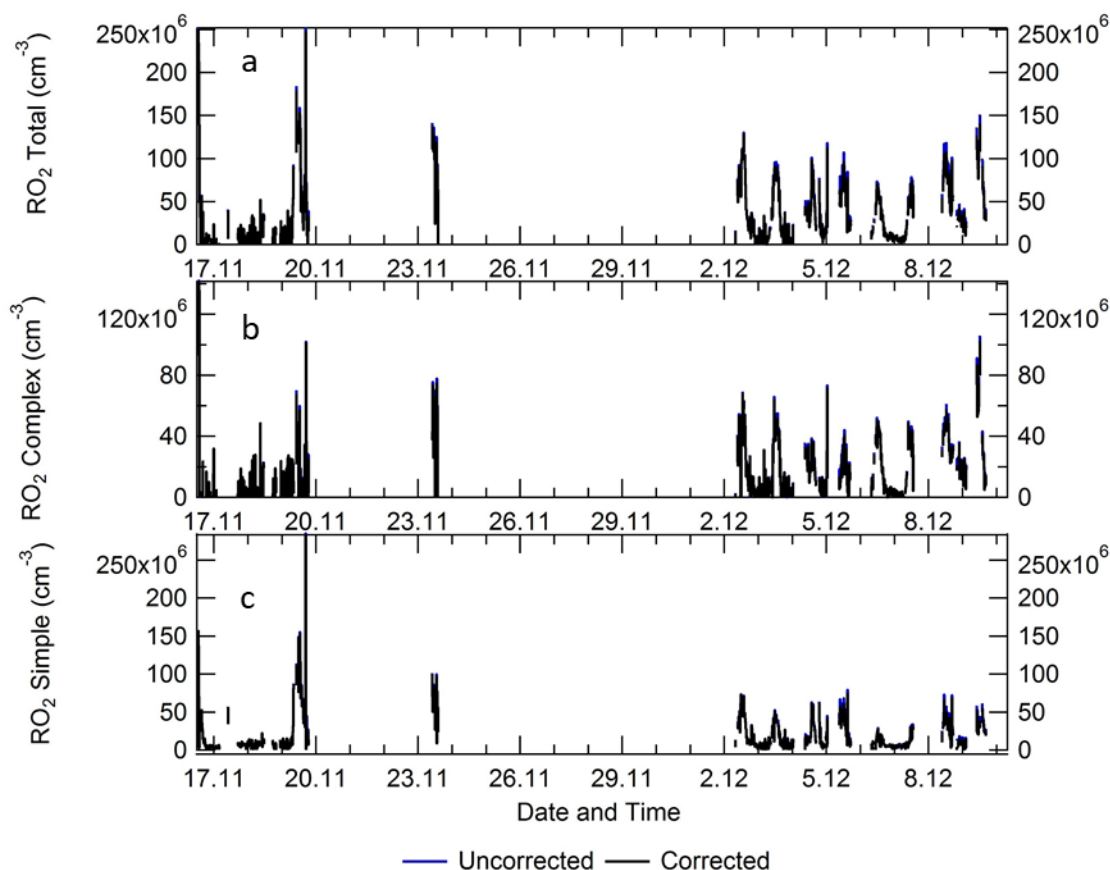


Figure S2. a) Timeseries comparison for measured total RO₂ (blue) and total RO₂ corrected (black) for the decomposition from HO₂NO₂ and CH₃O₂NO₂. b) Timeseries comparison for measured complex RO₂ (blue) and complex RO₂ corrected (black) for the decomposition from HO₂NO₂. c) Timeseries comparison for measured simple RO₂ (blue) and simple RO₂ corrected (black) for the decomposition from CH₃O₂NO₂.

S1.5 Exploring the sensitivity of the photostationary steady-state OH calculation to the HONO concentration.

The HONO concentration used to constrained both the model and the photostationary steady-state calculation was the suggested value by Crilley et al.(2019). During the campaign there was several HONO measurement present and, although the measurements agreed on temporal trends and variability ($r^2 > 0.97$), the absolute concentration diverged between 12 – 39%, the value suggested by Crilley et al. (2019) was the mean of the measurements. Since HONO is a primary source of OH the impact of the variable HONO concentration has been explored by increasing and decreasing the HONO by 40%, the results are shown in Figure S6. Figure S6 shows that the variation observed in the HONO measurements can increase/decrease the PSS up to 17% which is smaller than the error on the measured OH of ~26%.

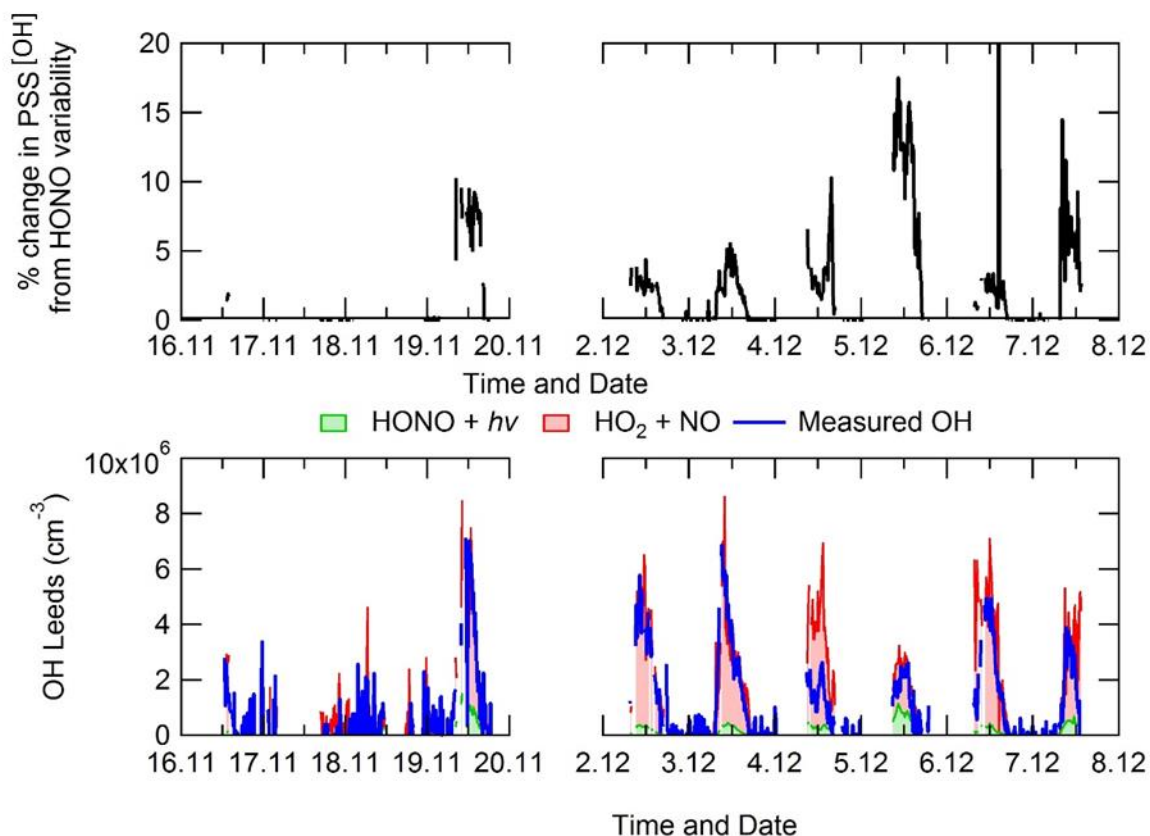


Figure S3. Top – Percentage change in the OH calculated from the PSS when the HONO is varied by 40%. Bottom – Comparison of the measured OH and the OH calculated from the PSS using the mean suggested value by Crilley et al. (2019).

S1.6 In-depth comparison of measured OH and OH calculated from the PSS on the 04/12 using measured and modelled OH reactivity.

On the 04/12/2016 the PSS calculation for OH is overpredicted by ~ 2.5 and the modelled OH reactivity is higher than the measured OH reactivity by an average of $\sim 14 \text{ s}^{-1}$. The modelled OH reactivity was used in the PSS calculation for OH and a comparison between the PSS calculation using measured and modelled kOH and measured OH is shown in Figure S7. Figure S7 shows that whilst using the modelled OH reactivity does reduce the calculated PSS OH, the PSS using modelled kOH still overpredicts the measured OH by a factor of ~ 2.4 . The large overprediction by the PSS suggests the differences between the PSS and measured OH on the 04/12/2016 stems from measurement problems and could be derived from issues with the OH, HO₂, HONO or NO measurements on this day.

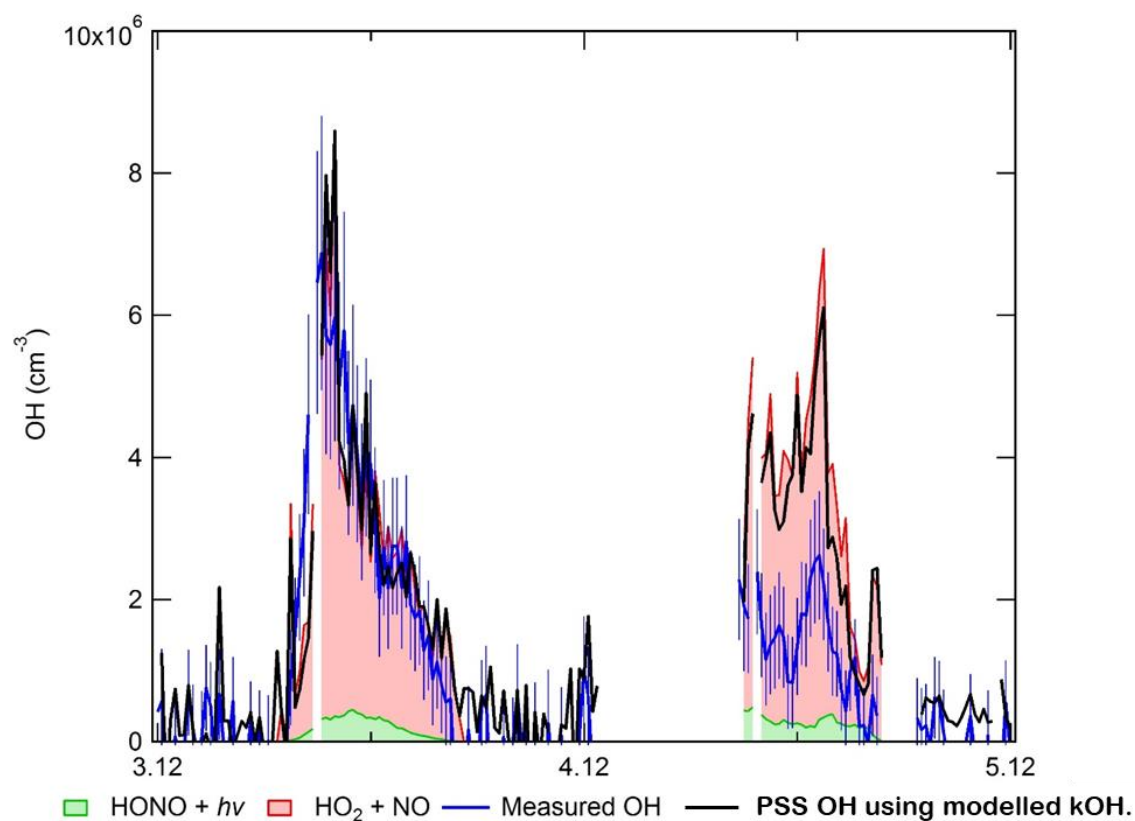


Figure S4. Comparison of measured OH (with errors, blue bars) with OH calculated from a photostationary steady-state (PSS) calculation using measured OH reactivity. The contributions towards OH production from HONO + hv (green) and HO₂ + NO (red) are shown, as well as the OH calculated using the PSS but with modelled OH reactivity (black).”

S1.7 The effects of the kRO₂ + NO rate constant on the modelled radical species

Other than CH₃O₂ and C₂H₅O₂, rate constants for the reaction of many other RO₂ + NO is based on structure activity relationships (SARs) in the MCM and is lumped to kRO₂NO and kAPNO (<http://mcm.leeds.ac.uk/MCM/>). The lumped rate constants kRO₂NO and kAPNO were both decreased by a factor of 2 and 10 to investigate the effects on modelled OH, HO₂ and RO₂. The model where the rate constant for RO₂ + NO was decreased by a factor of 2 is titled MCM-kRO₂-2, whilst the model where the rate constant was decreased by a factor of 10 is titled MCM-kRO₂NO-10.

The comparison of measured values with modelled values (MCM-base, MCM-kRO₂-2 and MCM-kRO₂-10) is shown in Figure S8. Figure S8 shows that on certain days (e.g. 19/11, 5/12 and 9/12) when the model (MCM-base) could not reproduce the measured values of RO₂ the discrepancy between the measurements and the MCM-kRO₂NO-10 model is almost reconciled. On these days the MCM-kRO₂NO-10 does not really change the OH or HO₂ concentration from the base model. On all days the MCM-base underpredicts the RO₂ concentration, and MCM-kRO₂NO-10 does decrease the gap between measurements and modelled, compared to MCM-base. MCM-kRO₂NO-2 does not significantly increase the total RO₂ concentration from MCM-base, unlike MCM-kRO₂NO-10. Since

changing the rates of $\text{RO}_2 + \text{NO}$ will be very dependent on the NO concentration, the ratio of measured:modelled radical concentration has been binned against the log of NO for MCM-base, MCM-kRO2NO-2 and MCM-kRO2NO-10 in Figure S9. Figure S9 shows similar results to the timeseries where at the lower concentration of NO (19/11, 5/12 and 9/12) the MCM-kRO2NO-10 can reproduce the RO_2 concentration. The results at higher [NO] show that decreasing the rate of $\text{RO}_2 + \text{NO}$ improves the agreement between measured:modelled RO_2 , especially for MCM-kRO2NO-10, but the observed RO_2 concentration is still underpredicted beyond 30 ppbv.

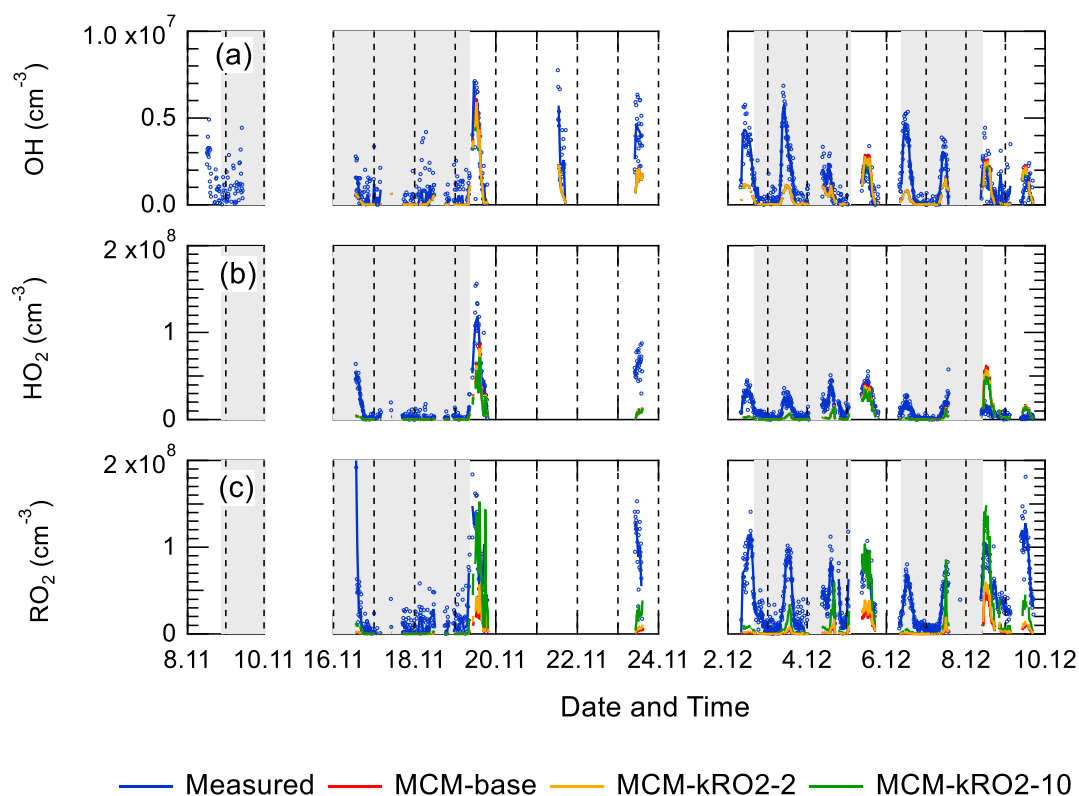


Figure S5. (a) Time-series comparison of measured values of OH with modelled OH concentrations from MCM-base, MCM-kRO23NO-2 and MCM-kRO2-10. (b) Time-series comparison of measured values of HO_2 with modelled HO_2 concentrations from MCM-base, MCM-kRO23NO-2 and MCM-kRO2-10. (c) Time-series comparison of measured values of total RO_2 with modelled total RO_2 concentrations from MCM-base, MCM-kRO23NO-2 and MCM-kRO2-10. The data sets are 15-minutes averaged.

The fact that the OH and HO_2 modelled concentrations do not change significantly for the models with reduced $\text{RO}_2 + \text{NO}$ rate constant highlights that the enhanced RO_2 radicals (in MCM-kRO2-10) are not recycling into HO_2 or OH, even though the agreement for the RO_2 concentration is improved for these models (MCM-kRO2NO-2 and MCM-kRO2NO-10). The lack of RO_2 recycling highlights that the RO_2 and RO radicals are terminating rather than propagating in the model.

This work highlights alternative chemistry and solutions must be applied for the two different NO regimes observed during the Beijing wintertime campaign. At high [NO] (above 10 ppbv) further

reductions in the RO_2+NO rate constant would be required to reconcile the model with observations. However, at NO mixing ratios below 10 ppbv, further reductions in the RO_2+NO rate constant would lead to the model overpredicting the RO_2 concentration.

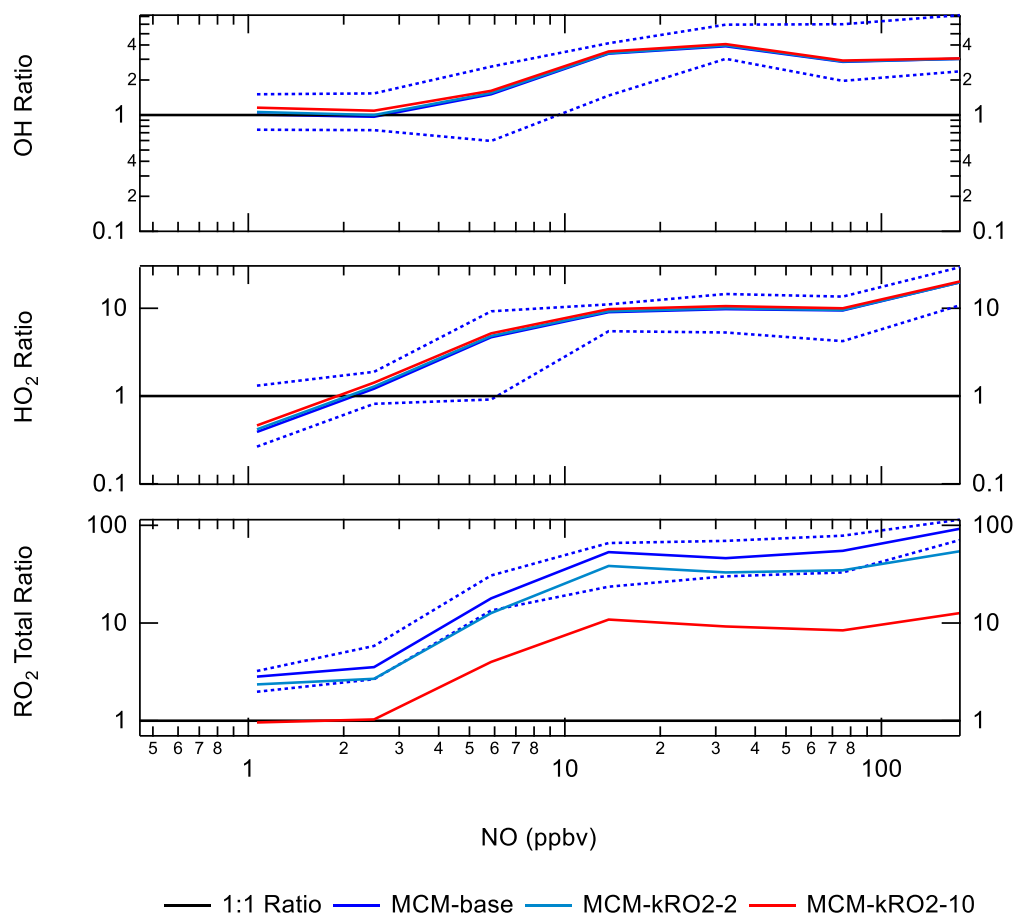


Figure S6. The ratio of measurement/model for OH (a), HO_2 (b) and RO_2 (c) across various NO concentrations for daytime values only ($j(\text{O}^1\text{D}) > 1 \times 10^{-6} \text{ s}^{-1}$). Light blue represents for results from MCM-kRO2NO-2, dark blue represents results from MCM-base and red represents results from MCM-kRO2NO-10.

S1.8 ClNO_2 and Cl concentration required to bridge the gap between measured and modelled total RO_2

Unfortunately, there were no ClNO_2 measurements during the winter campaign, and hence it was not possible to calculate a time series for Cl atoms formed from photolysis of ClNO_2 and to assess any additional RO_2 radicals generated. Using the model run where additional RO_2 source was added to reconcile the measurements and the model a rough calculation has shown that the ClNO_2 concentration would have to be on average ~ 5800 ppbv in order to close the gap between modelled and measured RO_2 . Figure S10 shows the average diel of the calculated ClNO_2 and Cl concentration with peak at 1.4×10^4 ppbv and 1.6×10^6 molecule cm^{-3} , respectively. The ClNO_2 and Cl concentration have been calculated using SE3 – SE5:

$$P'RO_2 = k_{VOC+Cl}[VOC][Cl] \quad S E 3$$

$$[Cl] = \frac{P'RO_2}{k_{VOC+Cl}[VOC]} \quad S E 4$$

$$[ClNO_2] = \frac{k_{VOC+Cl}[VOC][Cl]}{jClNO_2} \quad S E 5$$

where k_{VOC+Cl} is a generic rate constant to represents the reaction of all VOCs with Cl which in this case is $4 \times 10^{-12} \text{ molecule}^{-1} \text{ cm}^3 \text{ s}^{-1}$, [VOC] is the sum of the measured VOC concentration for the campaign and $P'RO_2$ is the calculated additional RO_2 used in MCM-PRO2 (see main paper section 4.2 for more details). The $ClNO_2$ required to bridge the gap between measured and modelled of RO_2 is ~ 3 orders of magnitude greater than the peak $ClNO_2$ concentration measured in suburban Beijing (2.9 ppbv) by Wang et al. (2018) suggesting that other additional primary source are needed in the model besides Cl chemistry .

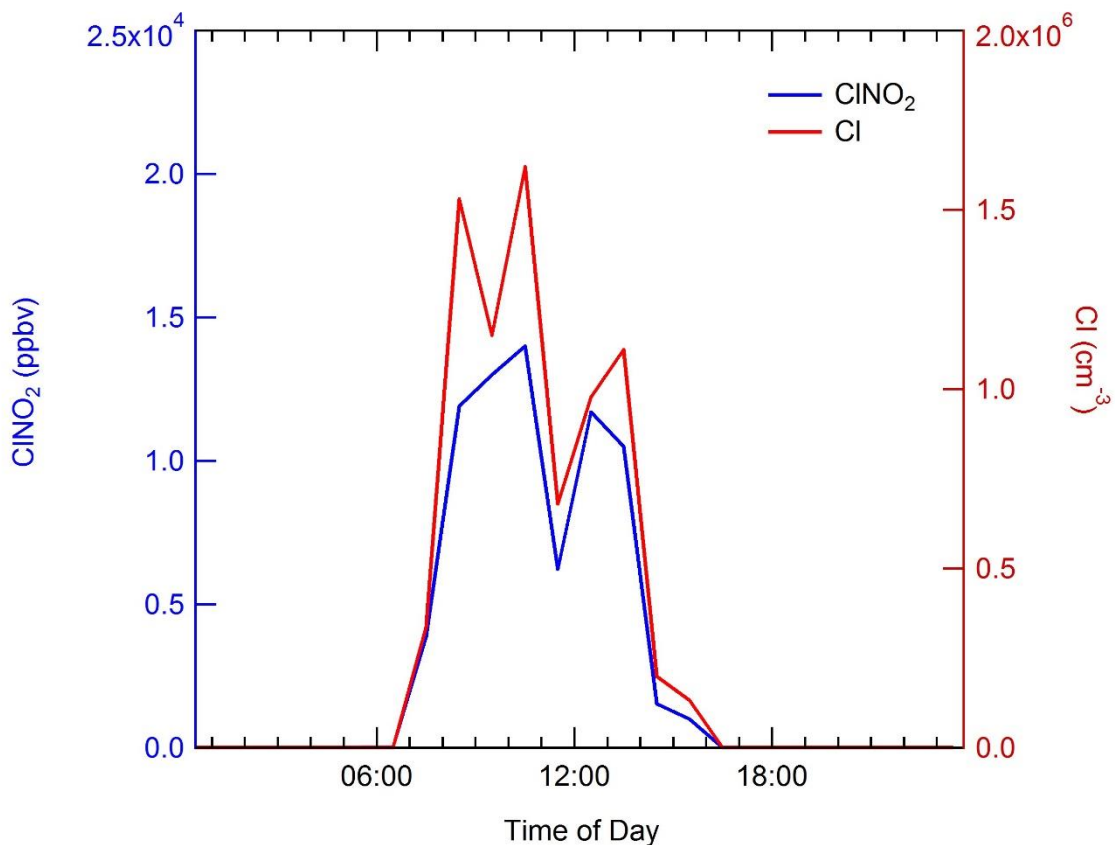


Figure S7. Average diel of the $ClNO_2$ and Cl atom concentration required to bridge the gap between measured and modelled RO_2 . The $ClNO_2$ and Cl concentrations have been calculated from the additional primary source of RO_2 added to the MCM-PRO2 model run, see section 4.2 in the main paper for more details.

References

- Ackermann, I. J., Hass, H., Memmesheimer, M., Ebel, A., Binkowski, F. S., and Shankar, U.: Modal aerosol dynamics model for Europe: Development and first applications, *Atmospheric environment*, 32, 2981-2999, 1998.
- Barth, M., Rasch, P., Kiehl, J., Benkovitz, C., and Schwartz, S.: Sulfur chemistry in the National Center for Atmospheric Research Community Climate Model: Description, evaluation, features, and sensitivity to aqueous chemistry, *Journal of Geophysical Research: Atmospheres*, 105, 1387-1415, 2000.
- Crilley, L. R., Karner, L. J., Ouyang, B., Duan, J., Zhang, W., Tong, S., Ge, M., Ge, K. T., Qin, M., Xie, P., Shaw, M. D., Lewis, A. C., Mehra, A., Bannan, T. J., Worrall, S. D., Priestley, M., Bacak, A., Coe, H., Allan, J., Percival, C. J., Popoola, O. A. M., Jones, R. L., and Bloss, W. J.: Intercomparison of nitrous acid (HONO) measurement techniques in a megacity (Beijing), *AMT*, 2019. 2019.
- Emmerson, K., Carslaw, N., and Pilling, M.: Urban atmospheric chemistry during the PUMA campaign 2: Radical budgets for OH, HO₂ and RO₂, *Journal of atmospheric chemistry*, 52, 165-183, 2005.
- Fuchs, H., Holland, F. and Hofzumahaus, A., 2008. Measurement of tropospheric RO₂ and HO₂ radicals by a laser-induced fluorescence instrument. *Review of Scientific Instruments*, 79(8), p.084104.
- Ge, X., He, Y., Sun, Y., Xu, J., Wang, J., Shen, Y., and Chen, M.: Characteristics and formation mechanisms of fine particulate nitrate in typical urban areas in China, *Atmosphere*, 8, 62, 2017.
- Huang, R.-J., Zhang, Y., Bozzetti, C., Ho, K.-F., Cao, J.-J., Han, Y., Daellenbach, K. R., Slowik, J. G., Platt, S. M., and Canonaco, F.: High secondary aerosol contribution to particulate pollution during haze events in China, *Nature*, 514, 218, 2014.
- Kanaya, Y., Cao, R., Akimoto, H., Fukuda, M., Komazaki, Y., Yokouchi, Y., Koike, M., Tanimoto, H., Takegawa, N., and Kondo, Y.: Urban photochemistry in central Tokyo: 1. Observed and modeled OH and HO₂ radical concentrations during the winter and summer of 2004, *Journal of Geophysical Research: Atmospheres*, 112, 2007.
- Kim, S., VandenBoer, T. C., Young, C. J., Riedel, T. P., Thornton, J. A., Swarthout, B., Sive, B., Lerner, B., Gilman, J. B., and Warneke, C.: The primary and recycling sources of OH during the NACHTT-2011 campaign: HONO as an important OH primary source in the wintertime, *Journal of Geophysical Research: Atmospheres*, 119, 6886-6896, 2014.
- Lee, J., Whalley, L., Heard, D., Stone, D., Dunmore, R., Hamilton, J., Young, D., Allan, J., Laufs, S., and Kleffmann, J.: Detailed budget analysis of HONO in central London reveals a missing daytime source, *Atmospheric Chemistry and Physics Discussions*, 15, 22097-22139, 2015.
- Lu, K., Fuchs, H., Hofzumahaus, A., Tan, Z., Wang, H., Zhang, L., Schmitt, S., Rohrer, F., Bohn, B., and Broch, S.: Fast photochemistry in wintertime haze: Consequences for pollution mitigation strategies, *Environmental science & technology*, 2019. 2019.
- Ma, X., Tan, Z., Lu, K., Yang, X., Liu, Y., Li, S., Li, X., Chen, S., Novelli, A., and Cho, C.: Winter photochemistry in Beijing: Observation and model simulation of OH and HO₂ radicals at an urban site, *Science of The Total Environment*, 685, 85-95, 2019.
- Mozurkewich, M.: The dissociation constant of ammonium nitrate and its dependence on temperature, relative humidity and particle size, *Atmospheric Environment. Part A. General Topics*, 27, 261-270, 1993.
- Ren, X., Brune, W. H., Mao, J., Mitchell, M. J., Leshner, R. L., Simpas, J. B., Metcalf, A. R., Schwab, J. J., Cai, C., and Li, Y.: Behavior of OH and HO₂ in the winter atmosphere in New York City, *Atmospheric Environment*, 40, 252-263, 2006.

Sun, Y., Wang, Z., Fu, P., Yang, T., Jiang, Q., Dong, H., Li, J., and Jia, J.: Aerosol composition, sources and processes during wintertime in Beijing, China, *Atmospheric Chemistry and Physics*, 13, 4577-4592, 2013.

Tan, Z., Rohrer, F., Lu, K., Ma, X., Bohn, B., Broch, S., Dong, H., Fuchs, H., Gkatzelis, G. I., and Hofzumahaus, A.: Wintertime photochemistry in Beijing: observations of RO x radical concentrations in the North China Plain during the BEST-ONE campaign, *Atmospheric Chemistry and Physics*, 18, 12391-12411, 2018.

Wang, X., Wang, H., Xue, L., Wang, T., Wang, L., Gu, R., Wang, W., Tham, Y.J., Wang, Z., Yang, L. and Chen, J., 2017. Observations of N₂O₅ and ClNO₂ at a polluted urban surface site in North China: High N₂O₅ uptake coefficients and low ClNO₂ product yields. *Atmospheric environment*, 156, pp.125-134.

Zaveri, R. A., Easter, R. C., Fast, J. D., and Peters, L. K.: Model for simulating aerosol interactions and chemistry (MOSAIC), *Journal of Geophysical Research: Atmospheres*, 113, 2008.